Aerodynamics of centrifugal compressors: An examination of the geometry of radial diffusers

Cockshutt, E.P.; Schaub, U.W.

Laboratory Memorandum (National Research Council of Canada. Division of Mechanical Engineering. Engine Laboratory); no. NRC-ENG-46, 1965-07

L.O. 14560A FILE M2-17-13.C-19 PREPARED BY E.P.C. & U.W.S CHECKED BY U.S.	NATIONAL RESEARCH COUNCIL DIVISION OF MECHANICAL ENGINEERING OTTAWA, CANADA LABORATORY MEMORANDUM SECTION Engine Laboratory	NO. NRC-ENG-46 PAGE 1 OF 32 COPY NO. 4 DATE July 1965

SECURITY CLASSIFICATION Open

SUBJECT Aerodynamics of Centrifugal Compressors:

An Examination of the Geometry of Radial Diffusers

PREPARED BY E. P. Cockshutt & U. W. Schaub

ISSUED TO Internal

SUMMARY

An analytic method of subsonic radial diffuser design is proposed and investigated, wherein the passages are designed to yield a fixed equivalent diffuser angle or rate of area increase. It is demonstrated in the two dimensional case that much more rapid diffusion can be achieved than with a vaneless diffuser.

Existing correlations of acceptable diffusion limits of straight-walled diffusers are combined with this purely geometric design method to generate optimum diffusers, assuming that the slight curvature of the passages does not appreciably affect the diffuser performance.

TABLE OF CONTENTS

LIST OF FIGURES

1.0 INTRODUCTION

In certain applications of the centrifugal compressor, notably in VTOL lifting schemes (Ref. 1.), the outside diameter of the installed compressor is of critical importance. In order to achieve reasonable diffusion, it is desirable to use a relatively large diffuser, but this is not compatible with a compact installation.

This has forced a re-examination of an old question -- for a specified diameter ratio (outside diameter over inside diameter), how should a radial diffuser be designed to achieve a maximum stall-free diffusion within this geometry. The problem specifically examined is, given the radial and tangential velocity components of the flow from a centrifugal compressor, by how much may the velocity be decreased in a radial diffuser, assuming typically that the flow discharges into an outlet plenum and that hence only the magnitude of the emerging stream velocity is significant.

It is recognized that the acceptable diffusion limit is not an absolute limit, but represents experience gathered from a number of different investigations; a detailed diffuser design would be expected to involve a re-examination of applicable data complemented by an experimental verification.

2.0 ANALYSIS

The basis for the following analysis is that the passages of a radial diffuser, such as is shown in the sketch below, have a radius of curvature which is large relative to a typical passage width. Hence the passage design may be guided by experience appropriate to straight-sided diffusers for incompressible flows.

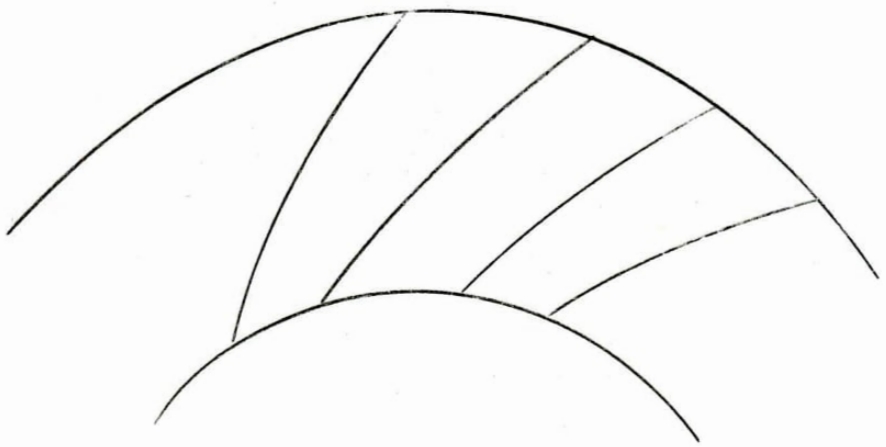

In particular, it is possible to so arrange the geometry of the passages, that a "constant equivalent diffuser angle" is achieved, i.e., the ratio of passage width increase to passage length increase remains constant, just as in the case of a straight-sided diffuser. The differential equation of the passage so defined is derived below.

2.1 Diffuser Passage Differential Equation

Consider an elemental portion of streamtube, extending from radius R to (R + dR), making an angle θ with the inner circle, and an angle $(\theta + d\theta)$ with the larger circle. See Figure 1.

If there are N streamtubes comprising the entire periphery of the diffuser, each streamtube intercepts an arc length of $(R\frac{2\pi}{N})$ on a circle. Since the streamtube makes an angle θ with the circle, the streamtube width at any given radius is

$$w = R\frac{2\pi}{N} \sin\theta \qquad (1.)$$

The increase in streamtube width is found formally as

$$dw = \frac{2\pi}{N} \sin\theta \, dR + R\frac{2\pi}{N} \cos\theta \, d\theta \qquad (2.)$$

The arc length of the streamtube element, by trigonometry, is

$$ds = \frac{dR}{\sin\theta} \qquad (3.)$$

These two quantities together define the equivalent diffuser angle, 2β, thus

$$2\beta = \frac{dw}{ds} = \frac{\frac{2\pi}{N} \sin\theta \, dR + R\frac{2\pi}{N} \cos\theta \, d\theta}{dR/\sin\theta} \qquad (4.)$$

Re-arranging

$$\frac{2\pi}{N} \sin^2\theta + \frac{2\pi}{N} \sin\theta \cos\theta \frac{R d\theta}{dR} = 2\beta$$

And separating variables

$$\frac{dR}{R} + \frac{\sin\theta \cos\theta \, d\theta}{\sin^2\theta - \frac{2\beta N}{2\pi}} = 0 \qquad (5.)$$

This differential equation sets out the relation between the local radius R, and the local angle with the

tangential direction θ, which must be fulfilled to achieve "constant angle" diffusion. This equation is readily integrated (the numerator of the second term being proportional to the derivative of its denominator), yielding the following relation

$$\frac{\sin^2\theta - \frac{2\beta N}{2\pi}}{\sin^2\theta_i - \frac{2\beta N}{2\pi}} = \left(\frac{R_i}{R}\right)^2 \qquad (6.)$$

It will be seen that, in addition to specifying the inlet angle and radius, one must also specify a dimensionless diffusion parameter.

$$DP = \frac{2\beta N}{2\pi} = \frac{2\beta}{2\pi/N}$$

$$= \frac{\text{Equivalent Diffuser Angle}}{\text{Streamtube Pitch Angle}} \qquad (7.)$$

One piece of significant information is available immediately, once the local angle has been determined -- this is the geometrical expansion which has taken place. The geometrical expansion is defined as follows:

$$\text{Geometrical Expansion} = \frac{\text{Local Passage Width}}{\text{Inlet Passage Width}}$$

$$= \frac{R \sin\theta}{R_i \sin\theta_i}$$

$$= \left(\frac{R}{R_i}\right)\left(\frac{\sin\theta}{\sin\theta_i}\right) \qquad (8.)$$

3.2. STREAMTUBE SPACE CURVE

While the integrated form of the diffuser equation (6) correlates the local angle, θ, with the local radius, R, it is convenient to define a space angle, α, which is the angular co-ordinate of any point under consideration, relative to its initial value.

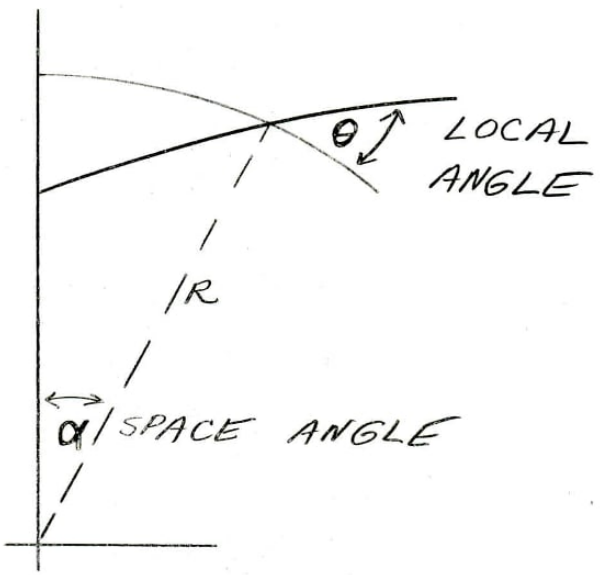

Referring back to Figure 1, it may be seen that for an incremental length of streamtube, the corresponding increment in the space angle, α, is

$$d\alpha = \frac{\text{Tangential Increment}}{\text{Local Radius}}$$

$$= \frac{\frac{dR}{\tan\theta}}{R} = \frac{dR}{R\tan\theta} \qquad (9.)$$

2.3 COMPUTER FORMULATION OF PROBLEM

In order to explore rapidly a large variety of diffuser configurations, the equations developed above were set up for computer evaluation. The problem as solved consisted of the following equations: -

$$ds = \frac{dR}{\sin\theta} \qquad (3.)$$

$$\frac{dR}{R} + \frac{\sin\theta\cos\theta d\theta}{\sin^2\theta - \frac{2\beta N}{2\pi}} = 0 \qquad (5.)$$

$$d\alpha = \frac{dR}{R\tan\theta} \qquad (9.)$$

Subject to the initial conditions

$$\left.\begin{aligned} \theta &= \theta_i \\ R &= R_i = 1.0 \\ \& \quad \alpha &= \alpha_i = 0° \end{aligned}\right\}$$

These equations have deliberately been left in the differential form, since that for the space angle is not convenient to integrate directly. They have been solved using the NRC IBM 1620 Mk II computer, using the Runge-Kutta-Gill method for solving simultaneous first order differential equations. A typical computer output sheet is shown as figure 2, for radius ratios between 1.0 & 4.0, fluid inlet angle of 20° and a diffusion parameter $\frac{2\beta N}{2\pi}$ of 0.5. The computed values of θ have been compared with those generated by the integrated relation (Eqn 6), and agree to at least 5 significant figures.

It will be noted that the computer output sheets also contain the geometrical expansion, as defined above, viz

$$\text{DIFNET} = \text{GE} = \left(\frac{R}{R_i}\right)\left(\frac{\sin\theta}{\sin\theta_i}\right) \qquad (8.)$$

Because the diffuser has been designed to yield a constant equivalent angle, 2β, the geometrical expansion may be correlated with the dimensionless passage length $\left(\frac{L}{W_1}\right)$, thus

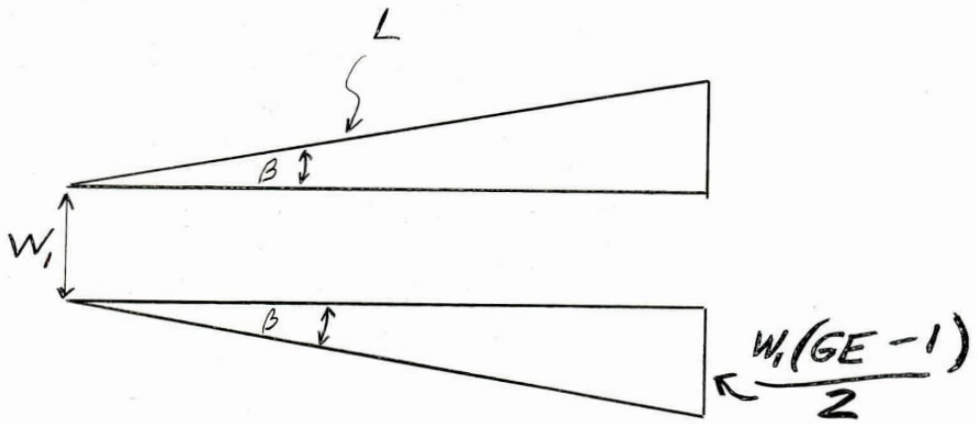

$$\beta \approx \sin\beta = \frac{W_1\ (GE-1)}{2L}$$

$$\text{or } \left(\frac{L}{W_1}\right) = \frac{GE-1}{2\beta} \qquad (10.)$$

This in turn may be correlated with the arc length, s, since

$$s = \left(\frac{L}{W_1}\right) W_1$$

$$= \frac{GE-1}{2\beta} \quad R_i \frac{2\pi}{N} \quad \sin\theta_i$$

$$s = R_i\ (GE-1)\ \frac{2\pi}{2\beta N}\ \sin\theta_i \qquad (11.)$$

Again the arc length as computed by finite difference integration has been found to agree to five significant figures with the value derived from the exact integrated result.

3.0 CALCULATED DIFFUSER GEOMETRIES

3.1 DATUM CASE

The computer results tabulated on Figure 2 are plotted in polar co-ordinates (R-α) in Figure 3; it will be noted that the diffusion parameter of 0.5 has been assumed to correspond to a value of 2β of 10°, and 18 passages (pitch angle of 20°). It could with equal accuracy be assumed to correspond to a value of 2β of 5° and 36 passages (pitch angle of 10°).

One point of particular interest is the relatively large radius of curvature of the diffuser passages defined by this analytic method - the correspondence to a straight-walled diffuser is hence very close.

The strongest curvature and highest expansion rates are found near the diffuser inlet, and hence this region sees the maximum departure from straight-wall diffuser experience.

A second point of some interest is that the local angle (θ) approaches a constant value of about 45° after changing rather rapidly at low radius ratios from its initial value of 20°. This may be seen from equation (6),

where as $\frac{R_i}{R} \rightarrow 0$

$$\sin^2\theta \rightarrow \frac{2\beta N}{2\pi} \quad \text{i.e.} \quad 0.5$$

whence $\theta \rightarrow 45°$

When this angle becomes constant, the curve becomes a

logarithmic spiral, and the expansion proceeds at a rate given by the radius ratio -- corresponding exactly to the vaneless diffuser case with free vortex flow.

It is also worth noting that for a radius ratio of 2.0, a geometric expansion of 3.72 is achieved. Providing this does not exceed the acceptable limits of diffusion, this represents a considerable gain over the geometric expansion of 2.0, which would be achieved with a logarithmic spiral or with a vaneless diffuser.

3.2 EFFECTS OF DIFFUSION PARAMETER

In Figure 4, the results of changing the value of the diffusion parameter are illustrated. If the passage spacing is held constant at 20°, the values shown correspond to diffuser angles of 20° and 5° respectively. With the diffuser angle of 20°, a straight diffuser passage results, yielding a geometric expansion of over 5, for a radius ratio of 2. With the diffuser angle of 5°, a long spiral-shaped passage results, yielding a geometric expansion of only 2.72 for a radius ratio of 2.

It is clear that the low diffuser angle is only marginally better than a log spiral passage -- the local angle θ converging towards a value of 30° at large radius ratios, as forecast by equation (6). The configuration with the large diffuser angle has a high expansion rate; it achieves a local angle approaching 90°, albeit rather slowly.

3.3 EFFECTS OF FLOW INLET ANGLE

In Figure 5, the effects of changing the diffuser inlet angle on the passage geometry are examined -- the upper curves being for an angle of 30° and the lower curves for an angle of 10°, both with an equivalent diffuser angle of 10°. With the higher inlet angle, the local angle is relatively constant, and the geometric expansion is not notably better than that with a logarithmic spiral. With the lower inlet angle, large amounts of expansion are achieved, typically a value of 7.12 being obtained with a radius ratio of 2.0. The tabulated values for this latter case are included as Figure 6., because they emphasize the extremely rapid expansion taking place near the start of the passage -- between R = 1 and R = 1.1 the local angle is approximately doubled and the geometric expansion is in excess of 2. Unless extremely close passage spacing is adopted, the flow may be inadequately constrained in this region.

4.0 OPTIMUM DIFFUSER DESIGN

4.1 PERFORMANCE CRITERION

In the foregoing, no attempt has been made to quantitatively justify the choice of diffusion parameter, and the component diffuser angle and passage pitch which comprise it. In this section, collective results of experimental investigations by various experimenters on straight diffusers are incorporated.

The basic piece of information is a curve of diffuser angle versus dimensionless diffuser passage length, (L/W_1), providing an acceptable diffusion limit. This curve has been plotted in Figure 7, on logarithmic co-ordinates, and is derived from reference 2, being applicable to flows of high turbulence.

As has been shown in equation (10), for a given diffuser angle specifying the non-dimensional passage length is the same as specifying the geometrical expansion so in the same Figure 7 is shown the limiting relation between diffuser angle and geometrical expansion.

Two points require emphasis. One is that the curves shown are applicable to straight diffusers, and their suitability to the curved diffusers considered here has not been demonstrated. The second point is that the curve in fact separates a flow regime of no appreciable stall from a flow regime of large transitory stall; clearly this only qualitatively defines an acceptable diffusion limit.

4.2 OPTIMUM DIFFUSER - FIXED RADIUS RATIO

The problem considered in this section is as follows: if the inside and outside radii are specified, and if the diffuser inlet angle is specified, what combination of passage number and diffuser angle will yield an optimum diffuser. Here the definition of an optimum diffuser is that arrangement which will produce a maximum geometrical expansion while falling within the acceptable diffusion limit.

Using equations (6) & (8), the geometrical expansion is readily computed as a function of the diffusion parameter. If, then, the number of passages is specified, a family of curves is generated relating diffuser angle with geometrical expansion - as is seen, in logarithmic co-ordinates, in Figure 8. To complete the examination, the diffusion limit as discussed in section 4.1 above is plotted on the same graph, and thus cases of large transitory stall can be separated out.

For the 20° inlet angle and 2.0 radius ratio selected, it is seen that a combination of high passage number and low diffuser angle will yield the highest geometrical expansion - with 18 passages, a maximum diffuser angle of 8° may be specified, yielding expansion of 3.35; alternately with 36 passages a maximum diffuser angle of 6° may be specified, yielding an expansion of 4.

Similar families of curves are shown for the same

radius ratio of 2.0, but for inlet angles of 10° and 30°, in Figures 9 and 10 respectively. With the 10° inlet angle, very large amounts of geometrical expansion are possible, but at very low diffuser angles - typically an expansion of 4.85 with a diffuser angle of 4 1/2°. This already represents some extrapolation of the available diffuser data, and does require some caution. With the 30° inlet angle, on the other hand, large numbers of passages are required to achieve any significant improvement over a simple logarithmic spiral - typically a geometrical expansion of only 2.77 is obtained with 18 passages and a diffuser angle of 11°.

4.3 OPTIMUM DIFFUSER - FIXED GEOMETRICAL EXPANSION

The problem considered in this section complements that considered above in 4.2: if a fixed expansion is to be produced by a diffuser and if the diffuser inlet angle is specified, what combination of passage number and equivalent diffuser angle will yield an optimum diffuser. The definition of an optimum diffuser in this case is the smallest radius ratio (most compact geometry) which can be used within the acceptable diffusion limit. Equations (6) & (8) may again be solved simultaneously for a fixed geometrical expansion, yielding the radius ratio as a function of the diffusion parameter:

From (6)
$$\frac{\left(\frac{R}{R_i}\sin\theta\right)^2 - \left(\frac{R}{R_i}\right)^2 \frac{2\beta N}{2\pi}}{\sin^2\theta_i - \frac{2\beta N}{2\pi}} = 1$$

From (8)
$$(GE)\sin\theta_i = \frac{R}{R_i}\sin\theta$$

whence
$$\frac{(GE\sin\theta_i)^2 - \left(\frac{R}{R_i}\right)^2 \frac{2\beta N}{2\pi}}{\sin^2\theta_i - \frac{2\beta W}{2\pi}} = 1$$

or
$$\left(\frac{R}{R_i}\right)^2 = \frac{\sin^2\theta_i\,(GE^2-1) + \frac{2\beta N}{2\pi}}{\frac{2BN}{2\pi}} \qquad (12.)$$

If the number of passages is specified, it is now possible to produce a curve of radius ratio as a function of equivalent diffuser angle -- one for each number of passages specified; this is done in Figure 11 for a geometric expansion of 4.0.

However, in Figure 7, it has been shown that the diffuser angle must be kept below 6° with this expansion, this limit is therefore superimposed on the curves generated by equation (12.)

As will be seen, with 18 passages, a radius ratio of at least 2.6 is required to keep the diffuser angle below 6°. By increasing to 36 passages, the radius ratio may be reduced 2.0, still achieving the geometrical expansion of 4.

A similar plot is shown in Figure 12 for an expansion of 3.0, with the inlet angle held constant at 20°. In this case the limiting diffuser angle is higher (9 1/2°) and the radius ratios from equation (12) are lower, with the result that much smaller diffusers are possible. Typically with 18 passages a radius ratio as low as 1.75 is permitted.

5. CONCLUSIONS

1. By using carefully chosen sets of parameters, much more rapid expansion can be achieved in a radial diffuser than would be possible in a vaneless diffuser.

2. The most rapid expansion rates, with respect to radius, occur near the diffuser inlet, so that it may be desirable to have an inner vaned portion with an outer vaneless annulus.

3. Studies of optimum diffusers indicate the extreme importance of maximum passage number, as the controlling variable in establising the limiting performance.

6. EXPERIMENTAL PROGRAMME

Should it appear desirable to verify and extend the analysis herein, the following comments are offered on an experimental programme.

It would be proposed to test a full annulus (rather than one or two passages), and to schedule removable vanes so that, typically, 9-18-36-vaned arrangements could be run. It would further be proposed to make the vanes in several discrete segments, so that the radius ratio could be changed over several values.

The flow would be provided by a conventional impeller, at low speed since compressibility is not of interest, with throttling used to adjust the diffuser inlet angle. Screens and/or a vaneless region might be desirable between the impeller and the test diffuser.

Flow visualization equipment would be highly desirable for these experiments. Velocities should however be made high enough to permit reasonably accurate pressure loss measurements.

7.0 REFERENCES

1. Cockshutt, E.P. and Lewty, P.J., Powerplants for VTOL Aircraft: A Preliminary Examination of Y-Axis Centrifugal Fans. Laboratory Memorandum NRC-ENG-44, March 1965

2. Kline, S.J., Abbott, D.E. and Fox, R.W., "Optimum Design of Straight-Walled Diffusers", Transactions of ASME, Vol. 81, Series D., p. 321, September 1959

3. Kline, S.J., "On the Nature of Stall", Trans. ASME, Sept. 1959, Vol. 81, Series D., Number 3, pp 305-320

4. Cockrell, D.J., and Markland, E., "Diffuser Design: A Review of Incompressible Diffuser Flow", Aircraft Eng., Oct. 1963, pp 286-292

Appendix A

On the Design of Subsonic Diffusers with Consideration of Observed Fluid Dynamic Phenomena

1. On Inlet Conditions

1.1 Boundary Layer at Entrance

The type of entrance boundary layer flow, while apparently not influencing the flow regime, affects critically both the pressure recovery and losses. Laminar inlet boundary layers separate easily when subjected to small pressure rises, and in the absence of re-attachment, cannot support satisfactory diffusion. Turbulent boundary layers can support considerable pressure rises because of their mass transfer properties (slow or backward moving fluid masses are either transported into higher velocity regions or are re-energized by momentum fed in from the higher mean velocity region. This mass transfer phenomenon represents a mixing loss - but it is a necessary agent in pressure recovery and in reducing total pressure loss from what it would have been for a completely stalled flow. It tends to decrease the history effect of the boundary layer (Ref. 2).

Considering turbulent entrance boundary layers, the stall patterns are only weakly dependent on Reynolds number (Ref. 3). Reynolds number in the range 6,000 to 300,000, at least, does not affect flow regime appreciably, but can have

considerable influence on losses and pressure recovery (Ref. 2). Thin boundary layers $\left(\frac{\theta}{W_1} < 0.01\right)$ tend to reduce diffuser loss and, providing that the diffuser is not stalled completely, the potential core (defined as a fluid region which has zero total pressure loss) extends to the full length of the diffusing passage (Refs. 2, 4). θ here is the momentum thickness and not the local angle defined in the main body of the text. There appears to be some evidence that pressure recovery varies more than total pressure loss with entry conditions (Ref. 2).

1.2 Velocity Profile of the Potential Core at the Entrance.

If a large area of inlet flow near a wall is deficient in total pressure (steady state or transient), e.g. a wake, large transitory stall (S. Kline's flow regime 2) will occur sooner than predicted by Kline's experimental data method (Ref.2). In the case of the radial diffuser design method described herein, this condition has to be anticipated because an impeller will necessarily precede the diffuser.

1.3 Inlet Aspect Ratio

The flow regime is not appreciately influenced by varying aspect ratio in the range $1/4 < W_1/h < 20$. Aspect ratio is thought to be an important variable in pressure recovery and loss (Ref. 2).

1.4 Mach Number

Raising inlet Mach number has an increasingly adverse effect on diffuser performance - particularly so with thick inlet boundary layers (Ref. 4). Increases in inlet Mach number up to 0.5, or somewhat higher, do not appear to alter the losses and hence performance - provided the design point is as much as 5 or 6 degrees below the normally acceptable diffusion limit at constant L/W_1. However, if the design is close to the normally accepted diffusion limit the losses appear to increase steadily with Mach number. The conservative units show flat performance up to conditions where shock waves and choking effects are encountered (Ref. 2). For radial diffuser designs of the proposed type the inlet boundary layer should be thin - hence Mach number effects on performance should be no worse than reported by Kline (see above) for thin inlet boundary layers.

1.5 Turbulence in the Potential Core

Increasing turbulence level and scale delays appreciable transitory stall and hence is beneficial for recovery (Ref. 2), presumably because turbulent mixing is aided.

2. On Correlating Flow Regime with Performance

Correlation of flow regime does not imply correlation of recovery value. Reynolds number, aspect ratio, inlet boundary layer (within limits) do not appreciably affect flow

regime, but they do affect recovery and losses (Refs. 2, 3).

At large diffuser angles, but in the region of no appreciable stall, the flow no longer follows the walls. Area ratio becomes a less significant variable as the diffuser angle increases (Ref. 2).

3. On Outlet Conditions (for No Transitory Stall Flow)

As the flow leaves the diffuser exit the velocity profile tends to be quite peaky. Adding some ducting (approximately 2 to 6 exit diameters would adequately suit the purpose (Ref. 4)), to the downstream end of the diffuser usually permits some further recovery since the profile tends to flatten out (Refs 2, 4). If the diffuser flow is dumped as is proposed in this design method, optimum pressure recovery will always be less than for the diffuser-short duct system (excepting cases where the diffuser angle is less than 7°)(Refs. 2 and 4).

4. Diffuser Performance

4.1 Loss Mechanism

Diffuser loss comprises three parts: dissipation due to wall shear, dissipation due to mixing (the greater of the two by about an order of magnitude), and a leaving momentum loss due to velocity peaking at the exit (see above) (Ref. 2).

4.1.1 Wall Shear

Wall shear in adverse pressure gradients, as is expected from considerations of the mean velocity profiles of the boundary layer, is found to be much lower than for equivalent pipe lengths (i.e. the flow regime defined as "no appreciable stall" often experiences a transient three-dimensional instability giving rise to streaks of back-flow at even mild pressure gradients); (Ref. 3). The spots of low energy fluid are confined to the boundary sub-layer while growing and are periodically swept away into the buffer and wake regions of the boundary layer (Ref. 3).

4.1.2 Reynolds Stress

A simple force analysis made by S. Kline demonstrates the presence and relative importance of the so-called Reynolds stress which, it turns out, is the only agent in the fluid stream that drags the boundary layer against the rising pressure and the wall shear (Ref. 3). The Reynolds stress becomes increasingly important as the flow approaches large scale separation (Ref. 2). This shear stress is seen therefore to actually aid the flow to diffuse - while acting at the same time to increase losses (mixing). In a turbulent boundary layer the dominant shear term is the Reynolds stress-it is several times the magnitude of the laminar shear term (Ref. 3). The Reynolds stress is increased by the appearance

of separation streaks at the wall. These streaks are little three-dimensional "bubbles" that cause sharp stream curvative (appearance of $\frac{\partial p}{\partial y}$ terms) which, in turn, increase the Reynolds stresses at greater distances from the wall (Ref. 3).

4.2 Loss Considerations

As large stalls begin to appear, whether transient or steady, both the mixing loss (which cannot be predicted analytically using conventional two-dimensional boundary layer theory) and the leaving momentum loss will rise sharply. The optimum pressure recovery is realized just as the large transient stalls appear - but at this point the diffuser pressure effectiveness has already degenerated.

The optimum pressure effectiveness is realized

when $$\frac{\partial C_{PR}}{\partial \beta} = \frac{C_{PR}}{C_{PR_{ideal}}} \cdot \frac{\partial C_{PR_{ideal}}}{\partial \beta}$$

or $$\frac{\partial C_{PR}}{\partial \beta} = \eta_p \cdot \frac{\partial C_{PR_{ideal}}}{\partial \beta}$$

The best pressure effectiveness is at $2\beta = 7°$ with L/W_1, = 25 to 30 where the 7° may represent a balance between wall friction and mixing losses such that their sum is minimized (Ref. 2).

4.3 Pressure Recovery Considerations

The foregoing observations have demonstrated, by implication, that pressure recovery must always be less than its corresponding ideal value. Optimum pressure recovery is

an impractical design goal because the resultant diffuser flows will pulsate and may stall completely when triggered by transient inlet conditions, and because the pressure effectiveness cannot be optimized simultaneously. Maximum pressure recovery values of 0.83 to 0.91 have been observed for diffusers with large L/W_1, and small expansion angle values, but a more reliable design recovery value appears to be 0.75 (Ref. 2). Furthermore, it appears prudent to avoid maximum recovery designs if inlet conditions are unknown, paricularly if diffuser angles greater than 12° are considered.

5. On Curved Diffusers

In the closure of Ref. 2, R. Dean cites examples of applying straight wall diffuser design methods to curved diffusers and diffuser-curved duct combinations - with excellent results. Particular reference was made of a 10° 4 to 1 area ratio conical diffuser followed by a 90° elbow. Here the pressure recovery was found to be 26% lower than predicted from straight wall diffuser data. The proposed design method features only mild diffuser centerline curvature and hence to use straight wall diffuser design rules would appear to be a good first approximation - provided the configurations are tested experimentally later.

NOMENCLATURE

A crossectional area

C_{PR} actual pressure recovery = $\dfrac{\frac{1}{A_2}\int_{A_2} p_2 dA_2 - \frac{1}{A_1}\int_{A_1} p_1 dA_1}{\frac{1}{A_1}\int_{A_1} q_1 dA_1}$

$C_{PR_{ideal}}$ ideal pressure recovery = $1-\left(\frac{A_1}{A_2}\right)^2$

h passage height

L wall length

p pressure

W passage width

y co-ordinate normal to wall surface

β diffuser wall angle, or 1/2 expansion angle

η_p pressure effectiveness $C_{PR}/C_{PR_{ideal}}$

θ momentum thickness of boundary layer

SUBSCRIPTS

1. inlet plane of diffuser

2. exit plane of diffuser

FIG. 1

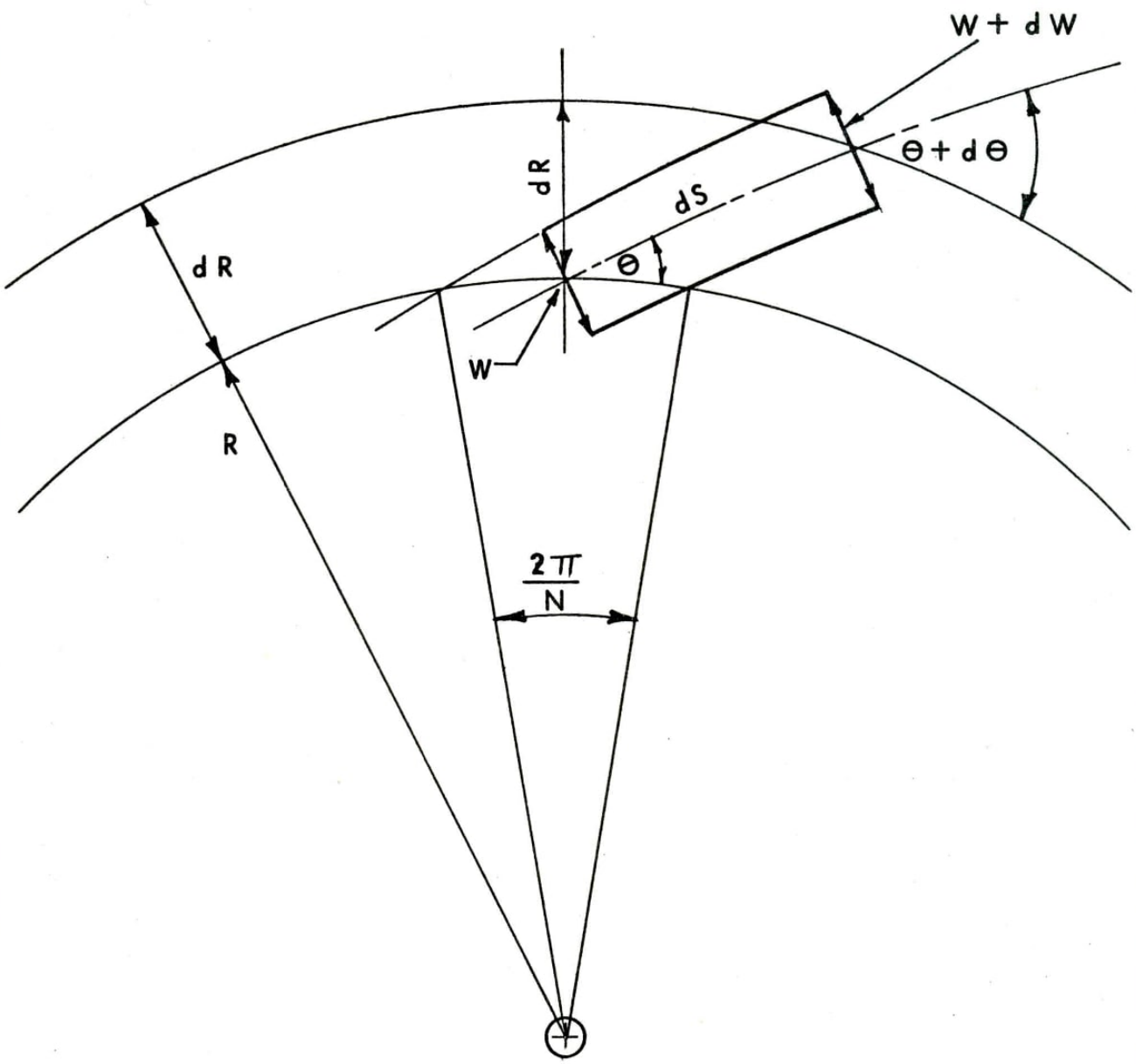

DIFFERENTIAL ANALYSIS OF RADIAL DIFFUSER GEOMETRY

FIG.2

RF	DELTA R	THETA	DIFPAR
4.0000	.1000	20.0000	.5000

R	THETA	ALPHA	S	DIFNET
1.0000	20.0000	0.0000	0.0000	1.0000
1.1000	25.3610	13.0255	.2582	1.3775
1.2000	28.9308	22.7311	.4769	1.6972
1.3000	31.5230	30.5933	.6753	1.9872
1.4000	33.4968	37.2504	.8612	2.2590
1.5000	35.0475	43.0479	1.0387	2.5185
1.6000	36.2942	48.1972	1.2101	2.7691
1.7000	37.3146	52.8381	1.3770	3.0130
1.8000	38.1620	57.0684	1.5403	3.2518
1.9000	38.8744	60.9595	1.7008	3.4865
2.0000	39.4795	64.5653	1.8591	3.7179
2.1000	39.9983	67.9273	2.0155	3.9465
2.2000	40.4467	71.0785	2.1704	4.1729
2.3000	40.8369	74.0454	2.3239	4.3973
2.4000	41.1787	76.8495	2.4763	4.6201
2.5000	41.4799	79.5089	2.6277	4.8415
2.6000	41.7466	82.0386	2.7783	5.0616
2.7000	41.9841	84.4514	2.9281	5.2806
2.8000	42.1963	86.7582	3.0773	5.4987
2.9000	42.3869	88.9683	3.2259	5.7160
3.0000	42.5586	91.0900	3.3740	5.9325
3.1000	42.7139	93.1305	3.5216	6.1483
3.2000	42.8549	95.0959	3.6688	6.3635
3.3000	42.9831	96.9919	3.8157	6.5782
3.4000	43.1002	98.8234	3.9622	6.7924
3.5000	43.2073	100.5949	4.1084	7.0061
3.6000	43.3057	102.3102	4.2543	7.2194
3.7000	43.3961	103.9731	4.4000	7.4324
3.8000	43.4795	105.5867	4.5454	7.6450
3.9000	43.5565	107.1540	4.6907	7.8573
4.0000	43.6278	108.6777	4.8357	8.0693

TYPICAL RADIAL DIFFUSER-COMPUTER OUTPUT LISTING

FIG. 3

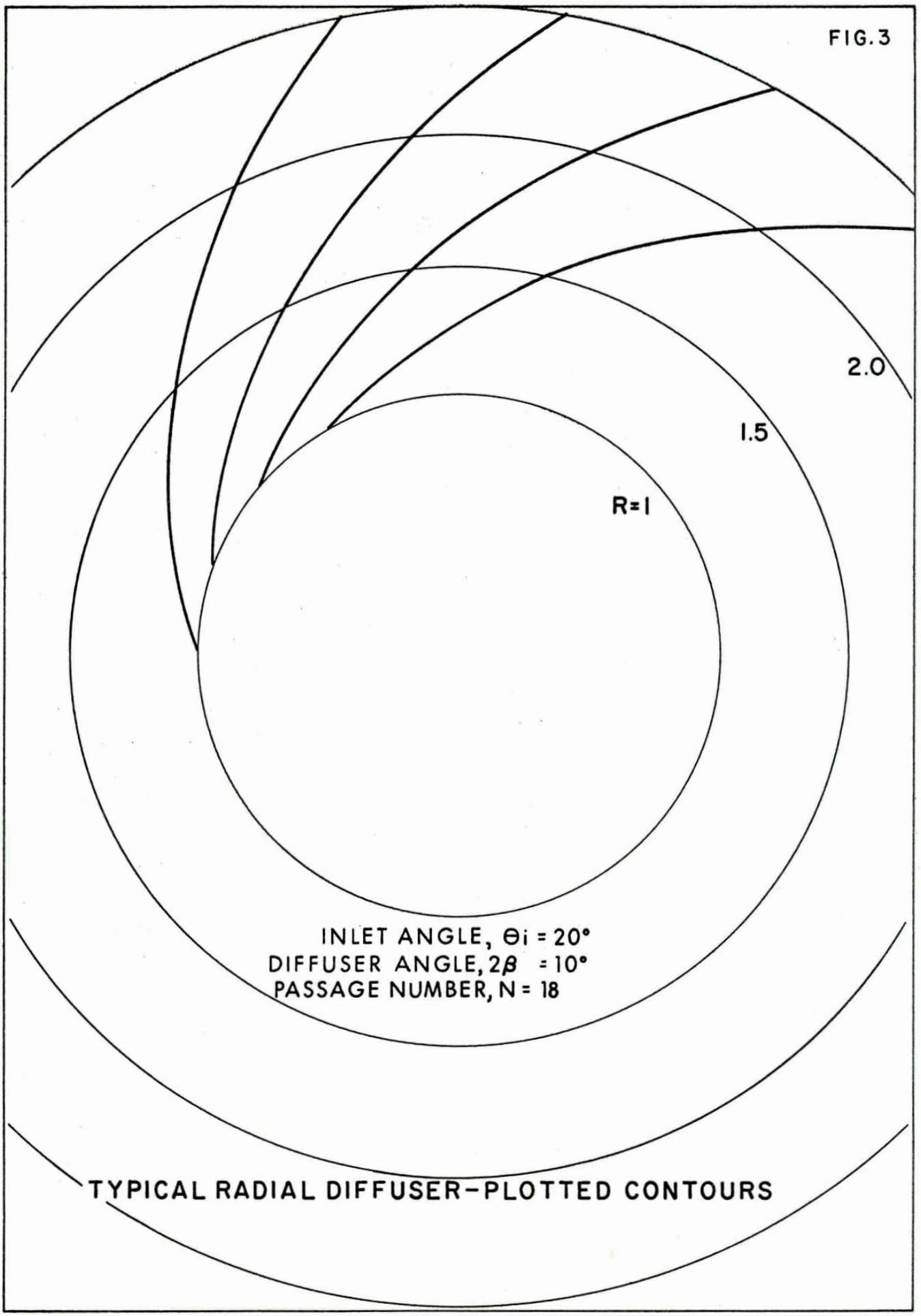

TYPICAL RADIAL DIFFUSER–PLOTTED CONTOURS

FIG. 4

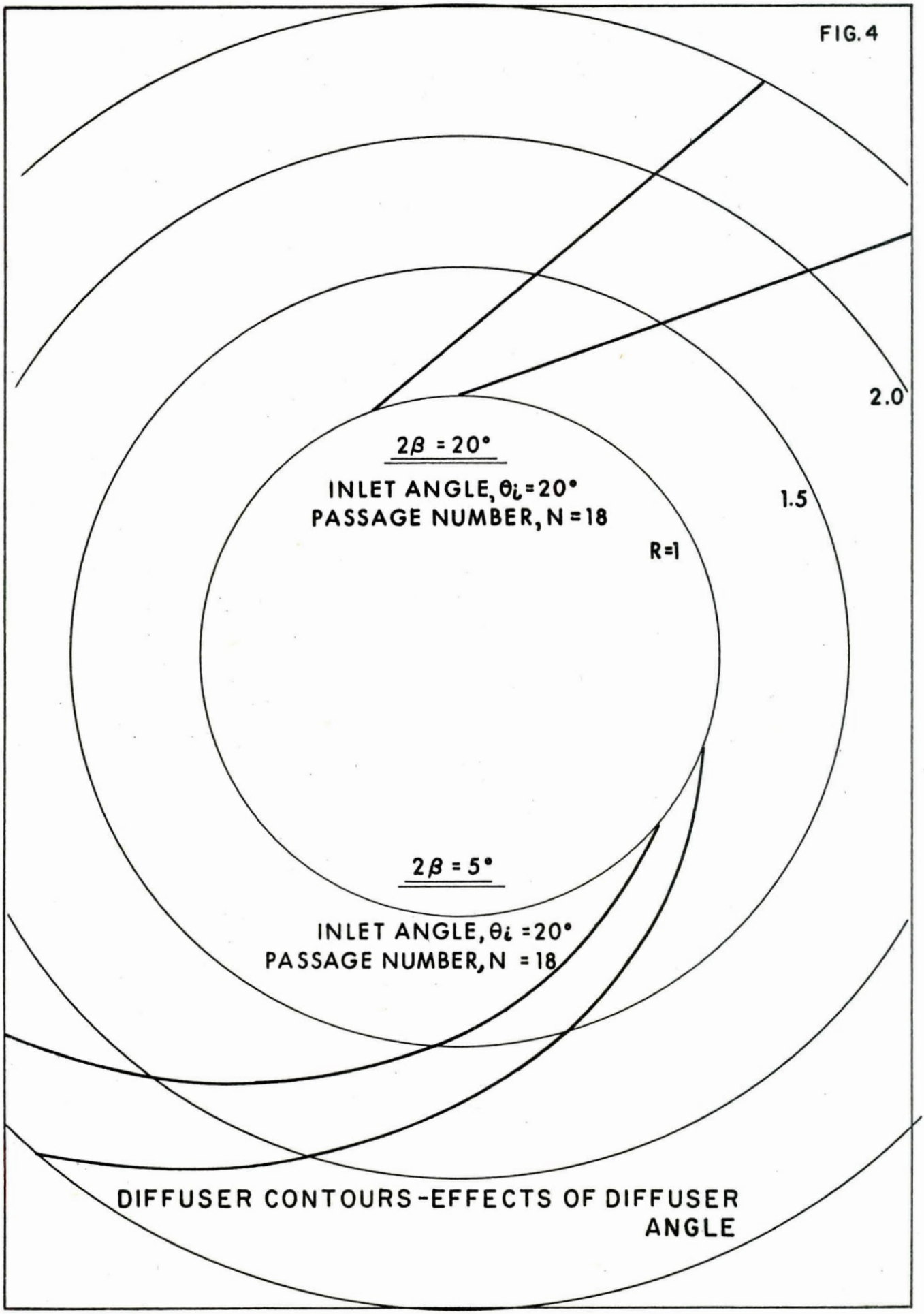

DIFFUSER CONTOURS - EFFECTS OF DIFFUSER ANGLE

FIG. 5

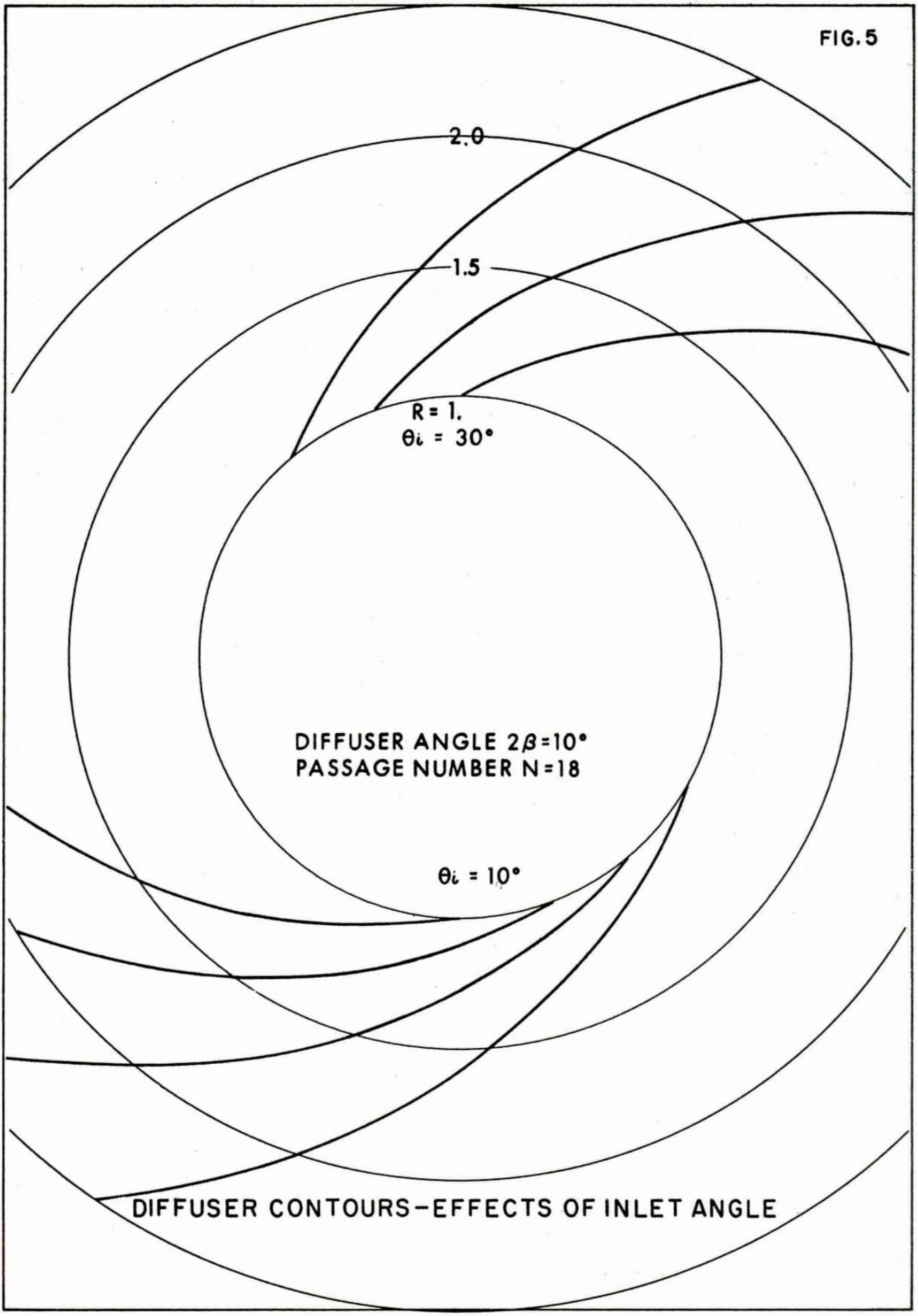

DIFFUSER CONTOURS–EFFECTS OF INLET ANGLE

FIG.6

RF	DELTA R	THETA	DIFPAR
4.0000	.1000	10.0000	.5000

R	THETA	ALPHA	S	DIFNET
1.0000	10.0000	0.0000	0.0000	1.0000
1.1000	19.5619	20.6428	.3893	2.1210
1.2000	24.6588	32.8795	.6540	2.8831
1.3000	28.1296	42.1054	.8785	3.5296
1.4000	30.6925	49.6295	1.0819	4.1152
1.5000	32.6712	56.0297	1.2721	4.6630
1.6000	34.2446	61.6222	1.4534	5.1849
1.7000	35.5231	66.6023	1.6282	5.6882
1.8000	36.5794	71.0999	1.7980	6.1773
1.9000	37.4642	75.2066	1.9641	6.6554
2.0000	38.2138	78.9892	2.1271	7.1247
2.1000	38.8551	82.4987	2.2875	7.5868
2.2000	39.4084	85.7742	2.4460	8.0430
2.3000	39.8895	88.8472	2.6027	8.4942
2.4000	40.3104	91.7427	2.7579	8.9412
2.5000	40.6810	94.4814	2.9119	9.3845
2.6000	41.0090	97.0805	3.0648	9.8248
2.7000	41.3009	99.5543	3.2167	10.2623
2.8000	41.5617	101.9150	3.3679	10.6974
2.9000	41.7957	104.1732	3.5182	11.1304
3.0000	42.0066	106.3379	3.6680	11.5615
3.1000	42.1972	108.4169	3.8171	11.9910
3.2000	42.3701	110.4171	3.9657	12.4190
3.3000	42.5275	112.3445	4.1139	12.8456
3.4000	42.6711	114.2046	4.2616	13.2710
3.5000	42.8026	116.0021	4.4090	13.6952
3.6000	42.9232	117.7413	4.5560	14.1185
3.7000	43.0341	119.4259	4.7027	14.5409
3.8000	43.1363	121.0596	4.8491	14.9624
3.9000	43.2308	122.6453	4.9952	15.3831
4.0000	43.3183	124.1860	5.1411	15.8032

COMPUTER OUTPUT LISTING–LOW INLET ANGLE

FIG.7

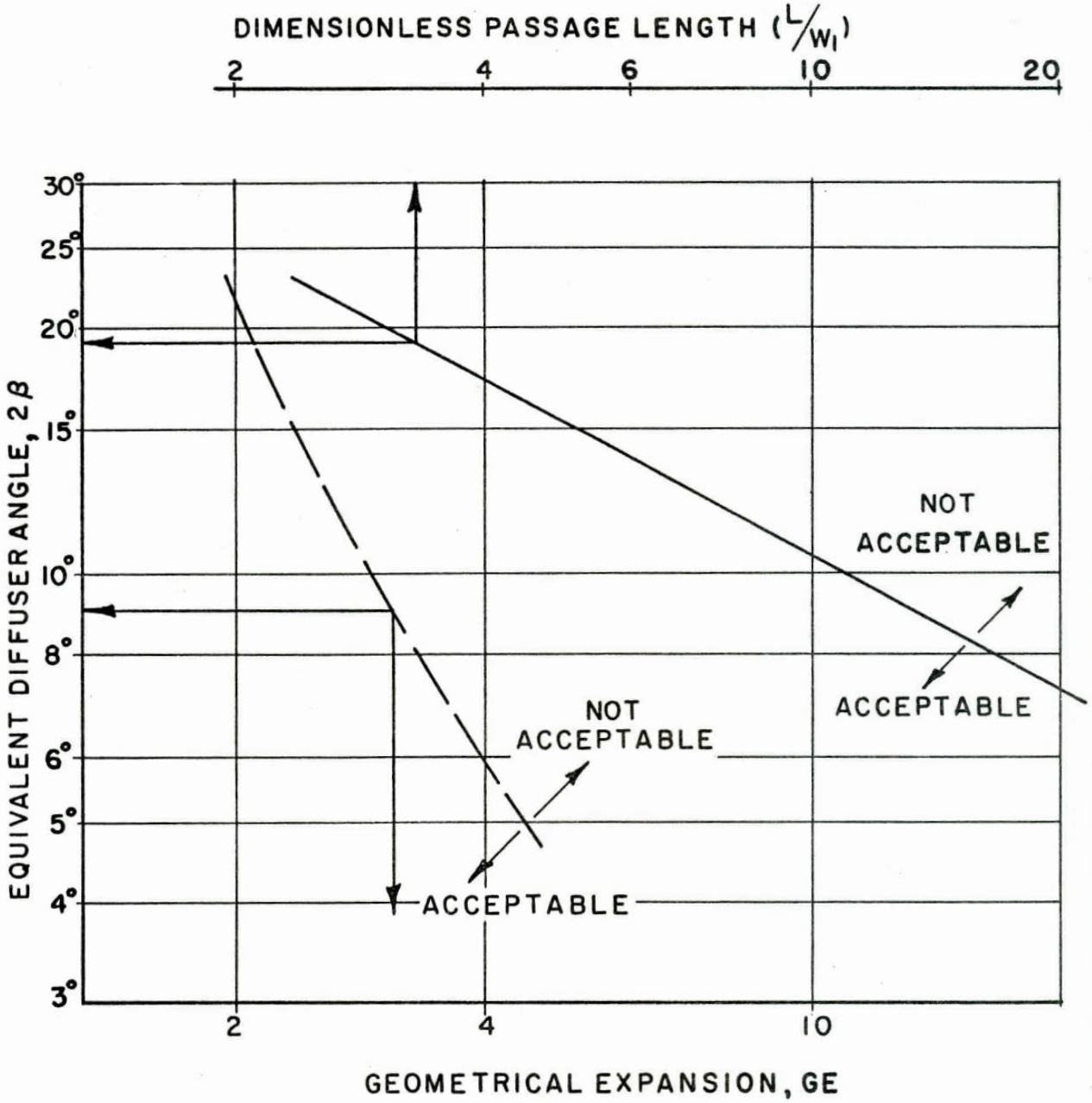

ACCEPTABLE DIFFUSION LIMIT (REF.2)

FIG. 8

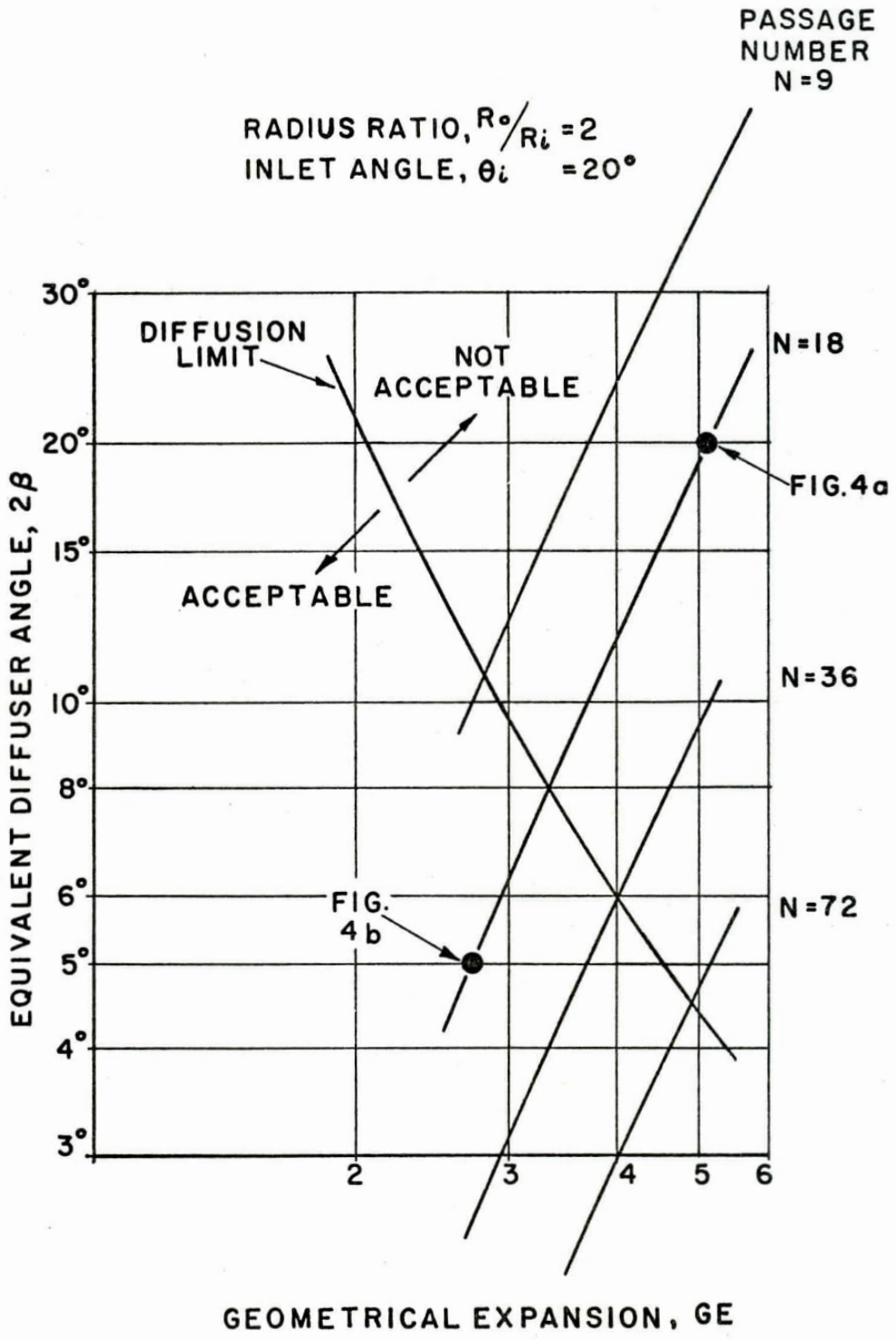

FIXED RADIUS RATIO DIFFUSERS — θ_i =20°

FIG.9

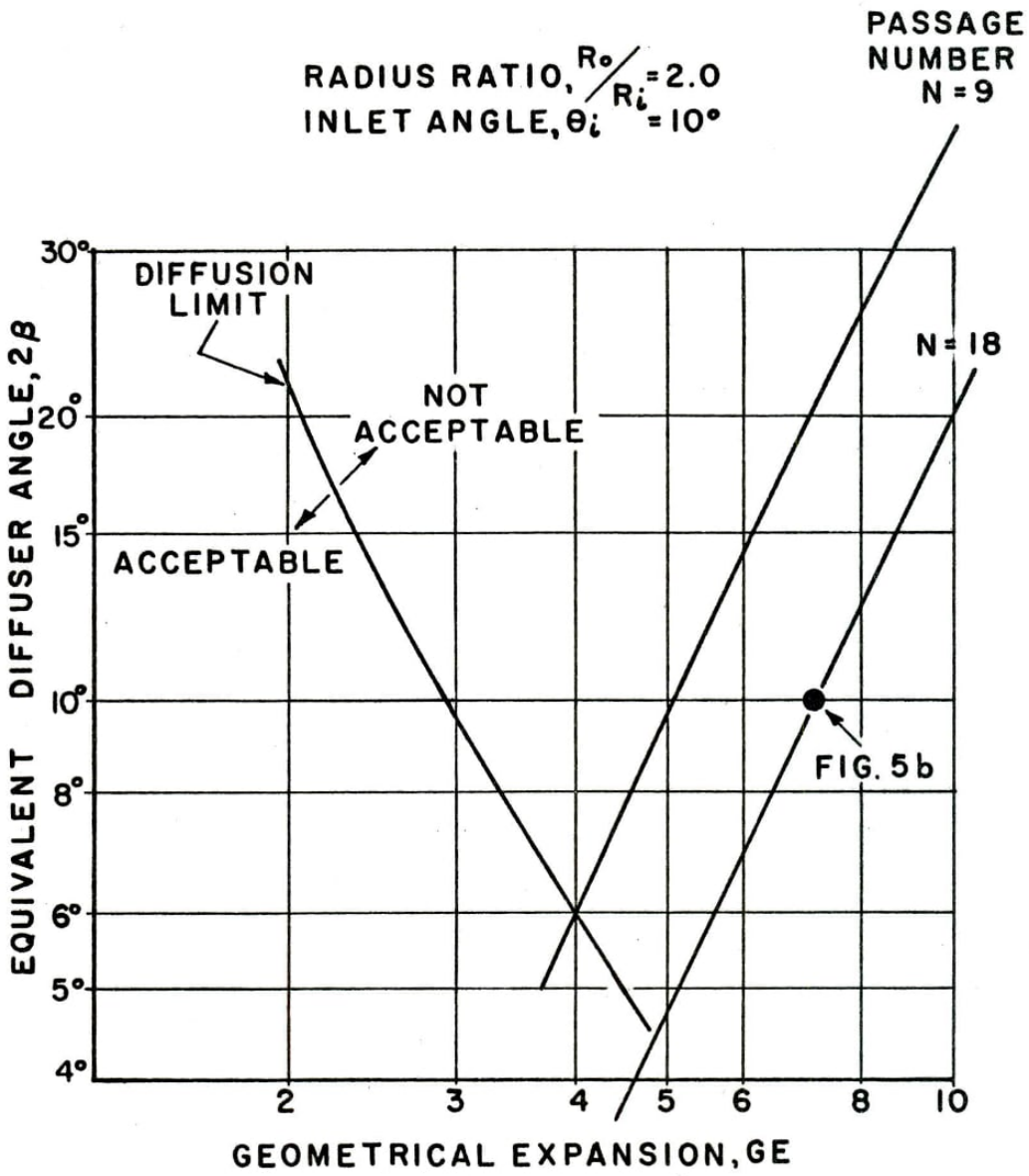

FIXED RADIUS RATIO DIFFUSERS-$\theta_i = 10°$

FIG.10

RADIUS RATIO, R_o/R_i = 2.0

INLET ANGLE, θ_i = 30°

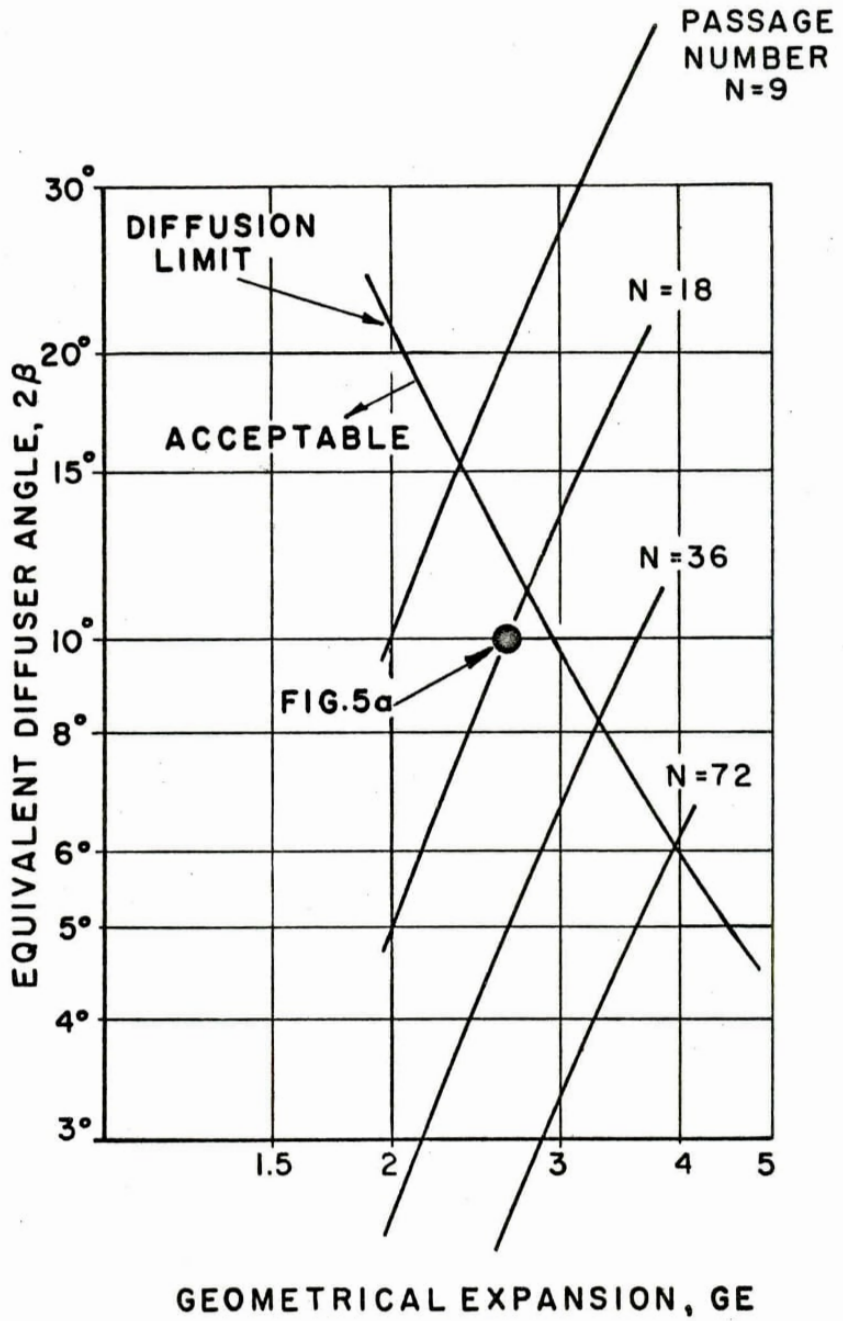

FIXED RADIUS RATIO DIFFUSERS – θ_i = 30°

FIG. 11

GEOMETRICAL EXPANSION, GE, =4.0
INLET ANGLE θ_i =20°

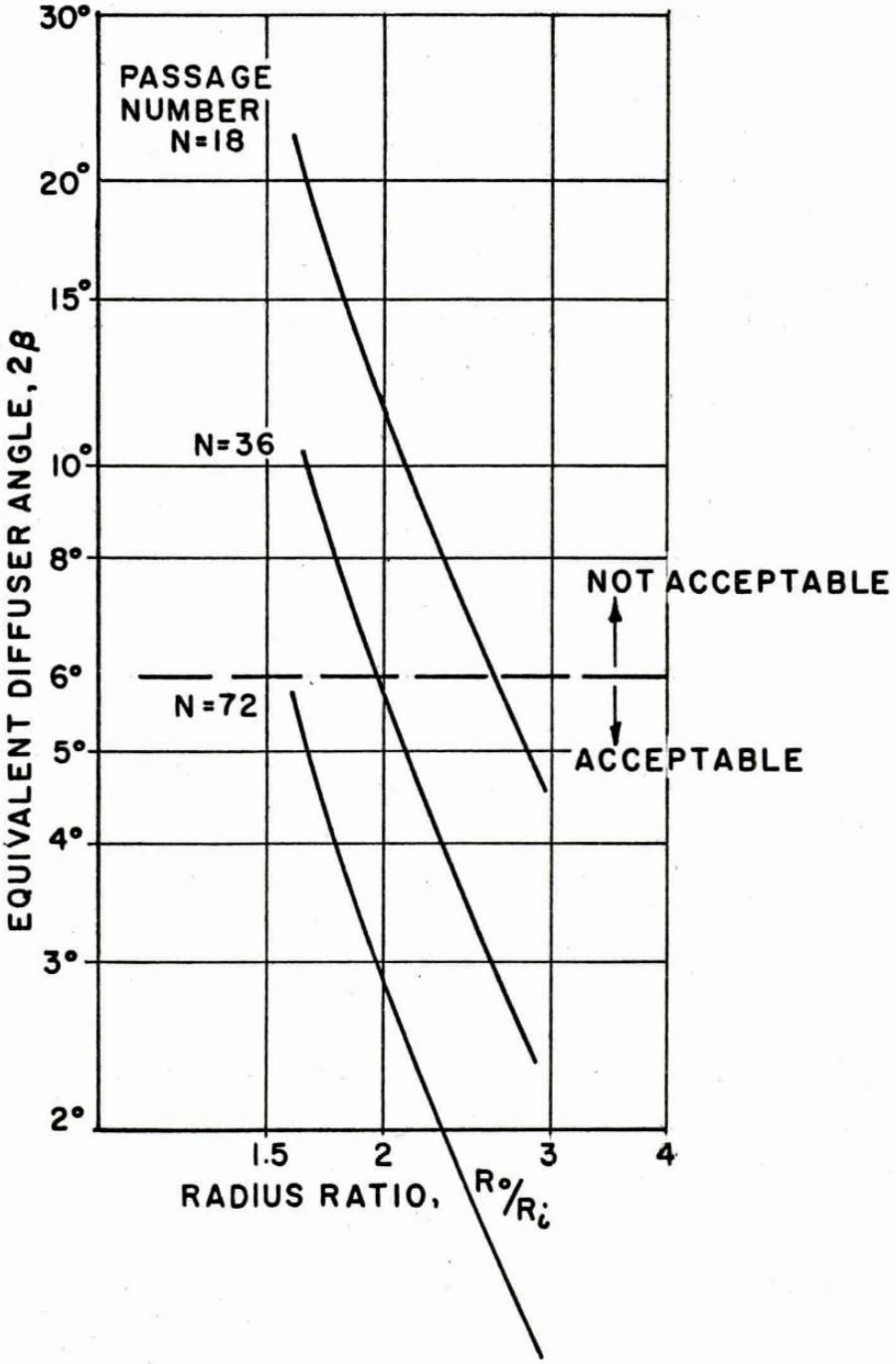

FIXED EXPANSION RATIO DIFFUSERS

FIG. 12

GEOMETRICAL EXPANSION, GE = 3.0
INLET ANGLE $\theta_i = 20°$

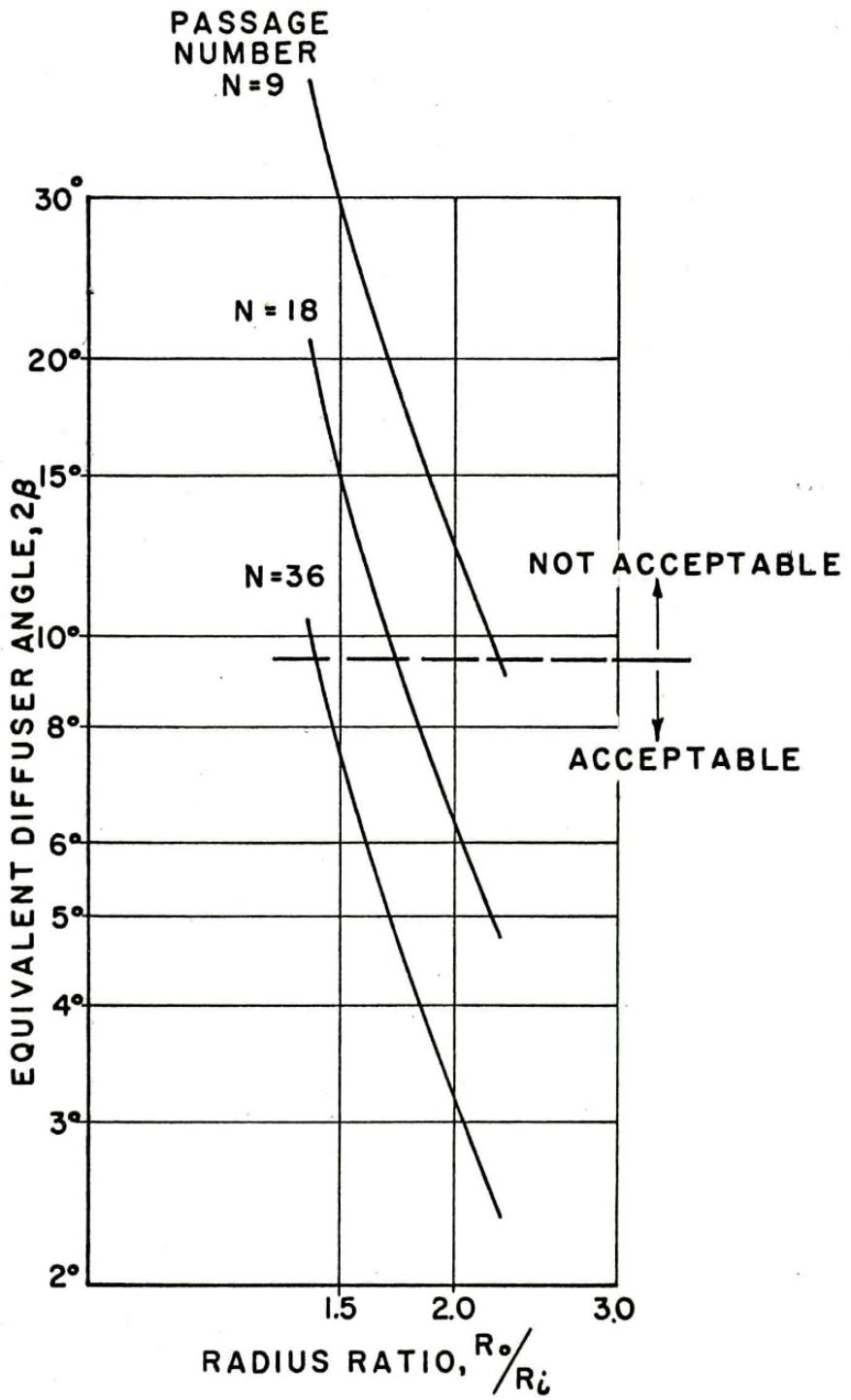

FIXED EXPANSION RATIO DIFFUSERS